Savenets, M., Pysarenko, L., Puhovkin, A., Miryuta, N., Pishniak, D., & Parnikoza, I. (2026). Microclimatological variability of incoming solar irradiance and snow cover availability near native vascular plants in the maritime Antarctic. *Ukrainian Antarctic Journal*, *24*(1), 29–49.
https://doi.org/10.33275/1727-7485.1.2026.756

Microclimatological variability of incoming solar irradiance and snow cover availability near native vascular plants in the maritime Antarctic

Mykhailo Savenets[1, *], Larysa Pysarenko[1, 2], Anton Puhovkin[2, 3, 4, 5], Natalia Miryuta[2], Denis Pishniak[2], Ivan Parnikoza[2, 6]

[1] Ukrainian Hydrometeorological Institute of the State Emergency Service of Ukraine and the National Academy of Sciences of Ukraine, Kyiv, 03028, Ukraine
[2] State Institution National Antarctic Scientific Center of the Ministry of Education and Science of Ukraine, Kyiv, 01601, Ukraine
[3] Masaryk University, Faculty of Science, Department of Geography, Kotlářská 267/2, Brno, 61137, Czech Republic
[4] Masaryk University, Faculty of Science, Department of Experimental Biology, A13–119, Brno, 62500, Czech Republic
[5] Institute for Problems of Cryobiology and Cryomedicine, National Academy of Sciences of Ukraine, Kharkiv, 61016, Ukraine
[6] National Historical and Architectural Museum "Kyiv Fortress", Kyiv, 01133, Ukraine

*** Corresponding author:** savenets@uhmi.org.ua, savenetsm@gmail.com

Abstract. Incoming solar irradiance is a crucial factor for the survival of native vascular plants in Antarctica, providing the primary energy source for local terrestrial vegetation growth. We analyse the microscale variability of incoming solar irradiance at the surface and evaluate its applicability as a proxy parameter for detecting snow cover availability in remote regions. The study is based on a network of 38 temperature and light sensors deployed within an established monitoring site in the Argentine Islands Kyiv Peninsula region during 2017–2025. At the microscale level, in sites where *Colobanthus quitensis* and *Deschampsia antarctica* occur, typical austral-summer irradiance values range from 200 to 500 $W \cdot m^{-2}$, with deviations of up to ±60% driven by local microscale conditions. We analysed the periods with near-zero measured irradiance, indicating stable snow cover that typically occurred from April to October. Being measured at the surface, solar irradiance disappearance can serve as a proxy for snow cover formation. The snow formation timing was relatively consistent, whereas the snowmelt timing varied significantly across sites. At the locations of native vascular plants distribution, the snow-free period varied in the range of 90 to 200 days, being dependent on microclimatological features. No statistically robust differences in the intra-annual irradiance cycle were detected between sites occupied by *C. quitensis* and *D. antarctica*; however, irradiance duration suggests a tendency for *C. quitensis* to preferentially occupy locations with longer irradiated periods. This study emphasises the importance of accounting for incoming solar radiation at the microscale and demonstrates the potential of light sensors as a proxy for assessing snow cover availability in remote Antarctic regions where direct observations are not possible.

Keywords: Antarctica, *Colobanthus quitensis*, *Deschampsia antarctica*, light intensity, microclimate, snowmelt

1 Introduction

Incoming solar radiation is an important factor in the formation of ecosystems in polar regions. Compared with other regions of the planet, the continuous polar day and night and the solar zenith angle are the primary drivers of the availability and variability of energy resources in these regions (Ding et al., 2019). Additionally, cloudiness is a key limiting factor for the intensity of surface solar irradiance (Láska et al., 2009; Zhang et al., 2019), playing an especially important role in coastal areas (Petkov et al., 2016). In the maritime Antarctic, cloud cover formation processes determine the spatial distribution of solar irradiance (Szymszová et al., 2025). At macro- and mesoscales, the role of other factors such as aerosol loading (di Carmine et al., 2005), stratospheric sulfur dioxide (Obryk et al., 2018), or others, is less influential in Antarctica.

From meso- to microscales, solar irradiance becomes strongly dependent on additional parameters, including environmental characteristics (Petkov et al., 2016) and terrain (Katurji et al., 2013). As drivers of vegetation distribution in Antarctica (Andrade et al., 2018), incoming solar radiation and its microclimatological variability are closely linked with terrain features, snow cover, and plants' distribution. Overall, the microscale conditions determine the characteristics of vegetation cover in the maritime Antarctic (Matos et al., 2024).

Solar irradiance is crucial for native vascular plants (*Deschampsia antarctica* É. Desv. and *Colobanthus quitensis* (Kunth) Bartl.) in terms of the biological dependence on ultraviolet (UV) radiation (Day et al., 2001) and its dual role in positive surroundings heating and negative radiation stress under low temperatures (Ramírez et al., 2024). Solar irradiance impacts vegetative growth and reproductive development (Day et al., 2001) and provokes biochemical responses (Barrera et al., 2020). However, the sparse spatial coverage of surface radiation observations often makes it difficult to directly link irradiance and biological data and to assess non-UV spectral effects, as well as the proportions of direct and diffuse solar radiation that influence canopy light interception, leaf temperature, and plant stress responses. Despite the more widespread availability of direct radiation measurements near the lichens (Pannewitz et al., 2003; Schroeter et al., 2011; Raggio et al., 2016), there are few long-term, direct measurements of radiation components at the micro-scales where native vascular plants grow.

The uncertainties and knowledge gaps in the variability of incoming solar irradiance at the microscale are sometimes difficult to address. This is because uncertainties still exist in global irradiance estimation and in the analysis of its long-term trends. In addition to biases among datasets (Zeng et al., 2022), trends in global irradiance have been reported as both increasing (Zeng et al., 2022) and decreasing (Bai et al., 2022). These estimates often exhibit some uncertainty and may not be fully reliable (Stanhill & Cohen, 1997). Therefore, any additional measurements and observations of solar radiation in Antarctica can provide very valuable information.

Establishing an observational site for native vascular plants on Galindez Island and in the Argentine Islands – Kyiv Peninsula region enables experimental observations of temperature and solar irradiance under the environmental conditions in which *D. antarctica* and *C. quitensis* grow (Miryuta et al., 2017). This data has already been used for analysing local temperature variability and relationship with standard meteorological variables (Savenets et al., 2023), as well as biometrical, biochemical, and ecological characteristics (Miryuta et al., 2025). The experimental observations showed that measurements of irradiance at the substrate surface within this monitoring site possibly can provide an indication of snow cover availability in remote areas where direct measurements are not feasible. This can be verified and compared with the most recent analyses of snow cover on Galindez Island based on other observational data (Shpyg et al., 2024; Khrystiuk et al., 2026).

The study aimed to analyse the intra- and interannual variability of incoming surface solar irradiance at the microscale level near native vascular plants and to assess its applicability as an indicator of snow cover availability. The results are structured as follows. After introducing the data and methodology, we present the quality control results, followed by an analysis of the diurnal and seasonal variability of incoming solar irradiance and its interannual changes. In the final part of the results, we assess the applicability of light logger data for snow cover identification, an important task for obtaining a proxy indicator when direct snow cover observations are not possible.

2 Data and methods

This study is based on the temperature and light logger data from the Bio-microclimatology Experimental Polygon / Monitoring Site (Miryuta et al., 2017; Savenets et al., 2023). In total, 38 loggers were deployed (see Fig. 1 and the description in Table A1). The study period covered 2017—2025. To distinguish seasons, the period from April of the previous year to March of the following year was selected (from 2017/2018 to 2024/2025), allowing both cold and warm periods to be included and ensuring consistency with the timing of logger replacement during expeditions, which usually ended in March. Since the 2024/2025 data had not been fully processed and quality-controlled, 2023/2024 is the last complete season available for calculations requiring a full year of observations.

The temperature and light logger data were recorded at 30-minute intervals. This interval was chosen as the main temporal resolution for analysing the diurnal cycle of irradiance. Thus, for daily statistical averages, a 30-minute step from 00:00 to 23:30 was used. In cases where loggers were programmed to record measurements slightly offset from 00 or 30 minutes, the values were assigned to the nearest 30-minute time step. For example, measurements recorded within the 46—60 min or 0—15 min intervals were assigned to the 00-minute mark, while measurements within 16—45 min were assigned to the 30-minute mark of the respective hour. This approach allowed statistical analysis across all years with available data without splitting the studied period into separate parts.

All data were recalculated to the most suitable representation of the sun's motion, mean local time of the Vernadsky Station, and all loggers (UTC-4) that allowed us to better reflect the physical conditions of irradiance at the site and construct an unbiased diurnal cycle.

Light measurements originally expressed in lux were converted to $W \cdot m^{-2}$ to align with the more commonly used units in meteorology. For this conversion, values in lux were multiplied by the conversion factor 0.0083.

During the light data processing, a limitation due to signal oversaturation at high irradiance was identified. In such cases, the measured irradiance could exceed the theoretical value of incoming solar radiation at the top of the atmosphere by 2—4 times. This phenomenon is referred to as "signal saturation". Under these circumstances, the irradiance values must be removed from the time series due to measurement errors. However, removing values during periods of high irradiance prevents any statistical analysis of radiation accumulation at the microclimatic scale, which is critical for studying vegetation response. To address this issue, a threshold value of 1300 $W \cdot m^{-2}$ was set. This value is lower than the theoretical solar irradiance at the top of the atmosphere (*i.e.*, lower than the value in the absence of atmospheric attenuation). At the same time, it approximates the maximum possible instantaneous irradiance in polar regions during a direct orientation of the logger toward the sunlight beam. Accordingly, time series were checked, and instantaneous values exceeding 1300 $W \cdot m^{-2}$ were set to this threshold.

The intra-annual distribution of irradiance intensity was analysed by calculating the multi-year mean diurnal cycle (30-minute time step) for each month of the year. The analysis of interannual irradiance distribution presents several challenges that often make proper statistical comparisons between different loggers and observation seasons difficult. These challenges include the abovementioned "signal saturation" and external influences on loggers (*e.g.*, animal impacts on logger overturning or shading), which may affect the measured solar radiation flux. As a result, statistical estimates based on absolute values can be biased, and calculating cumulative metrics may be impossible.

To overcome this issue for assessing inter-seasonal distribution, a relative indicator was introduced to reflect the average irradiance conditions during a season and to allow comparison of irradiance conditions at a given location across different seasons. The main idea is to apply double smoothing of extreme values, which are highly

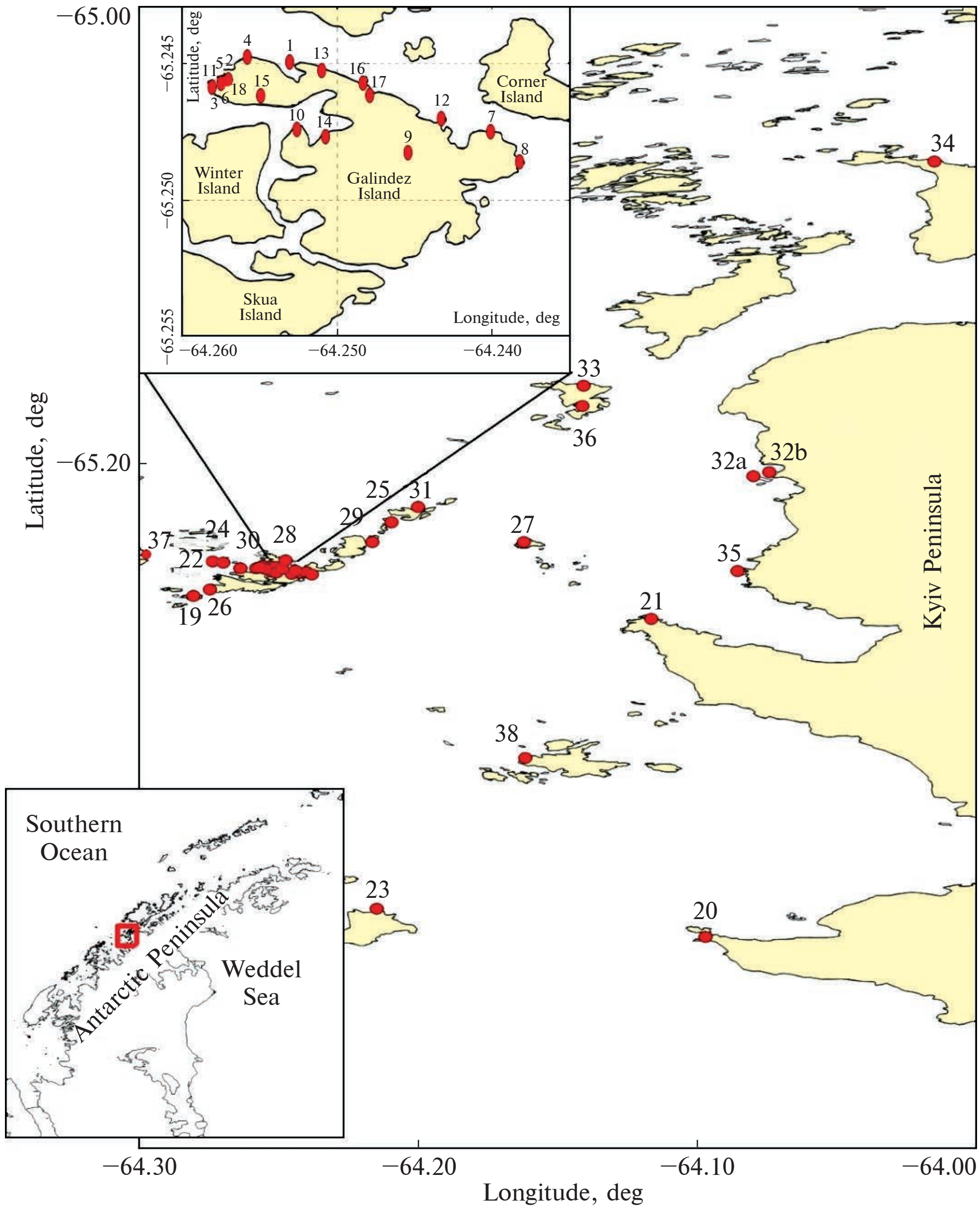

Figure 1. Study domain and the location of loggers within the Bio-microclimatology Monitoring Site on Argentine Islands Kyiv Peninsula region (numbers correspond to loggers in Table A1)

sensitive to statistical methods. In the first step, the mean daily cycle is calculated for each season using a 30-minute time step. In the second step, the mean daily cycle is calculated for the entire studied period. In the third step, the calculated parameters are averaged to obtain a single value of mean daily irradiance for the season and for the entire studied period. This double smoothing mitigates the negative impact of erroneous extremes on the statistical assessment of inter-seasonal distribution. In the fourth step, the ratio of seasonal to multi-year values is computed.

If the data series contains no erroneous values or cases of "signal saturation", the result of this procedure is equivalent to the ratio of the mean seasonal irradiance to the mean multi-year irradiance. For convenience, we introduce a metric called the Relative Intensity Index (*RII*). The entire four-step calculation algorithm can be expressed by a single equation

$$RII = \frac{\frac{1}{H}\sum_{h=0}^{H}\left(\frac{1}{D_y}\sum_{d=1}^{D_y} I_{y,d,h}\right)}{\frac{1}{H}\sum_{h=0}^{H}\left(\frac{1}{D}\sum_{y=1}^{Y}\sum_{d=1}^{D_y} I_{y,d,h}\right)} \approx \frac{\overline{I_y}}{\overline{I}},$$

where h is time of a day, H — total number of time steps in a day, d — day of a year; D_y — total number of days in certain season y; Y — number of years in studied period with data availability; $I_{y,\,d,\,h}$ — measured irradiance intensity for certain time h; $\overline{I_y}$ — mean irradiance intensity for the season y; $\overline{I}$ — mean irradiance intensity for the whole studied period.

Therefore, if the seasonal irradiance were close to average values, then *RII* would equal 1. If the seasonal *RII*, for example, equals 1.2, this indicates that the irradiance during that season was 20% higher than the mean level. Conversely, if the seasonal *RII* equals, for example, 0.8, this means that the average irradiance during that season was 20% below the mean. Therefore, this indicator can be used in conditions where there is a risk of erroneous values and after time series filtering, *i.e.*, it allows comparison of interannual changes in light intensity at the site where the logger is located. However, a limitation is that it cannot be used for direct comparisons between different locations; *RII* is only comparable over time under specific microclimatic conditions.

Logger light data can serve as a qualitative indicator of snow cover availability. As soon as solar radiation disappears, it indicates that the logger has been covered by snow or experienced another effect, such as dirt deposition, penguins building nests on the logger, the logger overturning, *etc*. The onset of snow can be distinguished by two combined criteria: consistency with temperature measurements and the timing of light disappearance. Clearly, if light disappears simultaneously across several loggers, this indicates snowfall, which, given the scale of the Bio-microclimatic Monitoring Site, represents substantial coverage.

At the same time, throughout the warm season, snowfall was frequent, followed by melting. Thus, during these periods, neither the vegetation nor the logger was under a stable snow cover. Determining the identification of a so-called "stable" snow cover (as opposed to short-term episodes) cannot be carried out using the methodology for air temperature. Consequently, to identify the dates of seasonal formation and melting of stable snow cover, the following methodology was applied.

Firstly, a threshold value of 10 W · m^{-2} was used to indicate the appearance of a layer that obstructs irradiance. The 10 W · m^{-2} threshold was based on the daily variation in solar irradiance on clear days during the warm season; *i.e.*, it corresponds to the intensity recorded by the loggers after sunset and, in some cases, throughout the entire night.

Secondly, to distinguish stable snow cover from temporary effects of synoptic-scale events, a 14-day period from the date of irradiance disappearance was used. Approximately 14 days corresponds to the duration of two synoptic-scale events, which excludes short-term episodes. The date of transition to stable snow cover is considered the initial date from which no irradiance was observed for the following 14 days. The date of disappearance of stable snow cover is defined as the first date after which irradiance either appears daily or begins to appear temporarily over the next 14 days. Part of the research on the variability of the dates of snow cover formation and melt has been conducted since 2019 to enable analysis of comparable logger datasets. During 2017—2018, the number of deployed loggers was considerably smaller, which made it impossible, for example, to include these years in the scatterplots presented.

To study the variability of transition dates, a box-and-whisker plot was used to show the median and mean values. The boundaries of the "box" represent the 25th and 75th percentiles, and the "whiskers" extend to the 5th and 95th percentiles. Outliers are values that fall outside the 5th and 95th percentiles.

3 Results and discussion

3.1 Results of data quality control. Statistics of "signal saturation"

As a result of the conducted quality control of the data for the studied period, in total 11723 values were identified that exceeded the theoretically possible irradiance, *i.e.*, measurements that recorded "signal saturation." These values were replaced with the upper threshold of 1300 W · m^{-2}.

Although such measurements are considered erroneous, their occurrence exhibited characteristic patterns of interannual variability and differed significantly across locations. Figure 2 shows the seasonal distribution of the relative number of irradiance values that reached "signal saturation" to the total number of measurements for the corresponding season at all studied locations.

First of all, it should be noted that the occurrence of "signal saturation" requires the presence of an intense solar radiation flux. Therefore, all such measurements appeared only during the summer season under predominantly clear skies. Consequently, both the seasonal and geographical distributions largely reflect the territory's thermal conditions. For example, at the coldest site "Radio", "signal saturation" was observed extremely rarely. In contrast, at loggers located in warmer areas, the frequency of erroneous data increased. Figure 2 shows that the highest number of erroneous values was recorded for the "Berth.", "Guczny", "Col. St.", "Indic.", and "Eight low." loggers, among others.

In certain seasons at specific sites, the number of measurements that reached "signal saturation" exceeded 250 values. The maximum percentage of such values reached up to 1.6% of all measurements. Although the number of these values may seem small, their absolute magnitudes differ so significantly from the theoretical limit of irradiance intensity that they introduce substantial errors into any statistical calculations. Therefore, when working with solar irradiance data, quality control is essential. Similarly, it is impossible to simply remove these values without replacing them with realistic ones, as this would underestimate the most significant contribution of available radiation resources.

Overall, during the studied period, the highest number of erroneous values was observed at the "Guczny" site, where 1022 unrealistic measurements were recorded, accounting for 1.1% of all time series data. More than 500 erroneous measurements were also identified at the "Berth.", "Eight low.", "Indic.", "Black.", and "Col. St." loggers, accounting for over 0.6% of the total number of measurements.

Considering that loggers under "signal saturation" cannot record realistic environmental values, it is recommended that in future research, when such values are detected, the corresponding temperature data should also be filtered. Such data quality control will prevent statistically biased estimates. In cases where removing these values makes analysis impossible (for example, when assessing the accumulation of thermal resources), it is recommended to replace them with a threshold that reflects realistic environmental conditions.

3.2 Intra-annual distribution of incoming solar radiation

The location of the Bio-microclimatology Monitoring Site is characterised by a well-pronounced seasonality of incoming solar radiation and a typical diurnal cycle associated with the alternation of day and night. In general, during daylight hours of the austral summer, long-term mean irradiance may exceed 500 W · m^{-2}. Instantaneous values, as noted above, can exceed 1000 W · m^{-2}.

In December–January, a sharp increase in radiation intensity is observed between 7:00 and

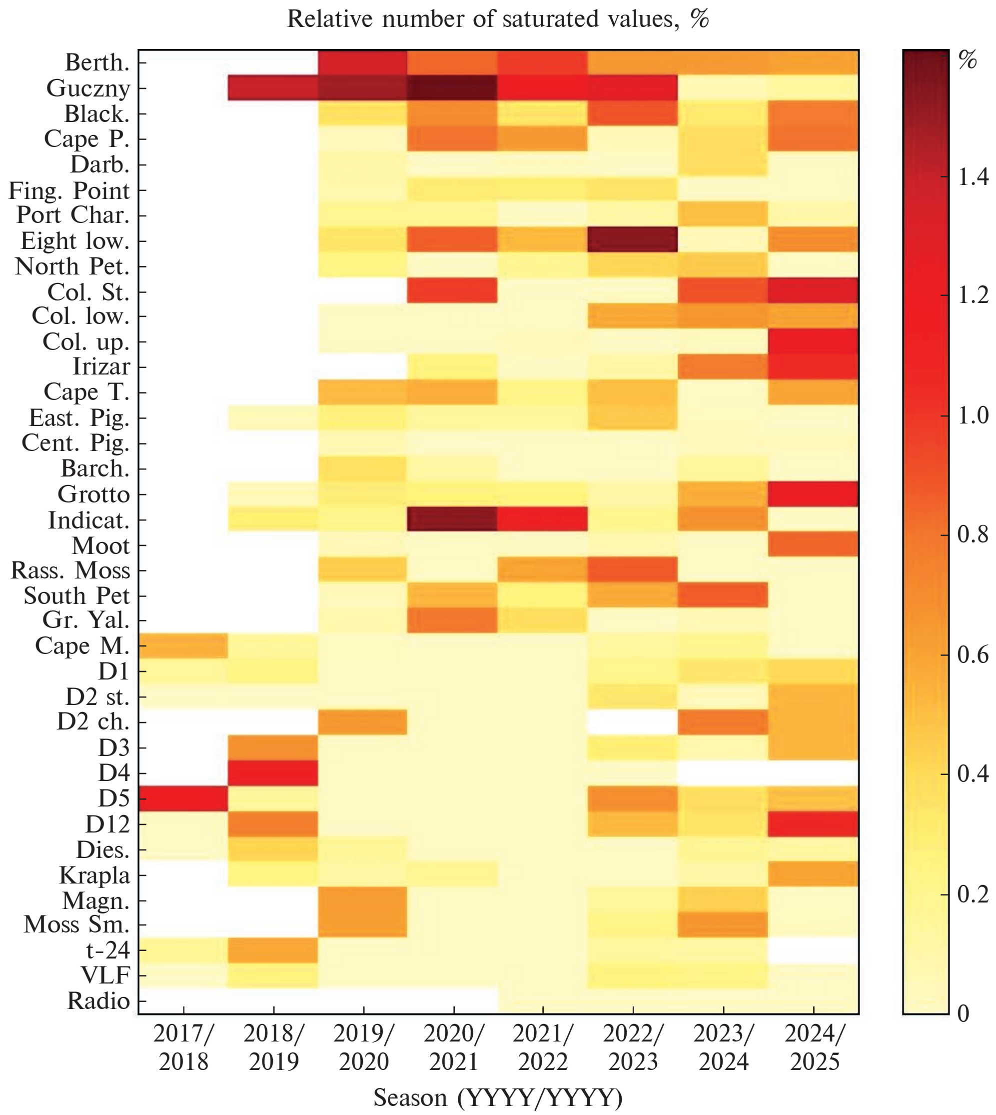

Figure 2. Inter-annual changes of the fraction (in %) of saturated values in the time series (white indicates data absence)

8:00 a.m. local (UTC-4), when irradiance rapidly rises from 50–70 W · m^{-2} to 80–170 W · m^{-2}, depending on the logger location (Fig. 3). Peak values are reached during daytime hours between 11:00 and 14:00, depending on microrelief characteristics and the degree of horizon obstruction. A similarly rapid decrease in solar irradiance intensity is observed between 17:30 and 18:30.

In March–April, a sharp change in the intensity of solar radiation reaching vegetation occurs due to the formation of a stable snow cover. From May to October, irradiance intensity averages zero, interrupted only near the transitional seasons.

Figure 3 presents the loggers with the highest ("Guczny") and lowest ("Radio") irradiance intensities, clearly indicating substantial variability in incoming solar heat across microrelief sites, even when these sites have similar orientation. Even considering the absence of vegetation at the "Radio" site, the lowest recorded long-term mean daytime summer incoming solar irradiance at vegetated sites does not exceed 180 W · m^{-2} (*e.g.*, the "Moot" logger in Fig. A2).

Figures A1 and A2 in the Appendix show the intra-annual distribution for all analysed loggers, separately for *C. quitensis* (Fig. A1) and *D. antarctica* (Fig. A2). As shown, the distribution of irradiance intensity is highly variable. At first glance, *C. quitensis* appears to be located under higher irradiance than *D. antarctica*; however, no robust statistical evidence supporting this assumption was found. In absolute values, the variability is considerable, and the presence of less irradiated sites for *D. antarctica* may simply reflect a larger number of loggers deployed for this species and, consequently, a broader range of environmental conditions represented.

3.3 Inter-annual distribution of incoming solar radiation

Despite the same external forcing of incoming solar irradiance and atmospheric attenuation at the spatial scale of the monitoring site, micro-scale environmental conditions can significantly affect the interannual variability of irradiance reaching the plants (as the loggers are located in close proximity to vegetation).

Figure 4 shows the distribution of the *RII* for all loggers over the period 2017—2024. A relatively lower incoming solar radiation at some sites does not necessarily correspond to similar patterns at other sites. For example, during the 2021/2022 season, irradiance intensity at the "Port Char.", "Col.

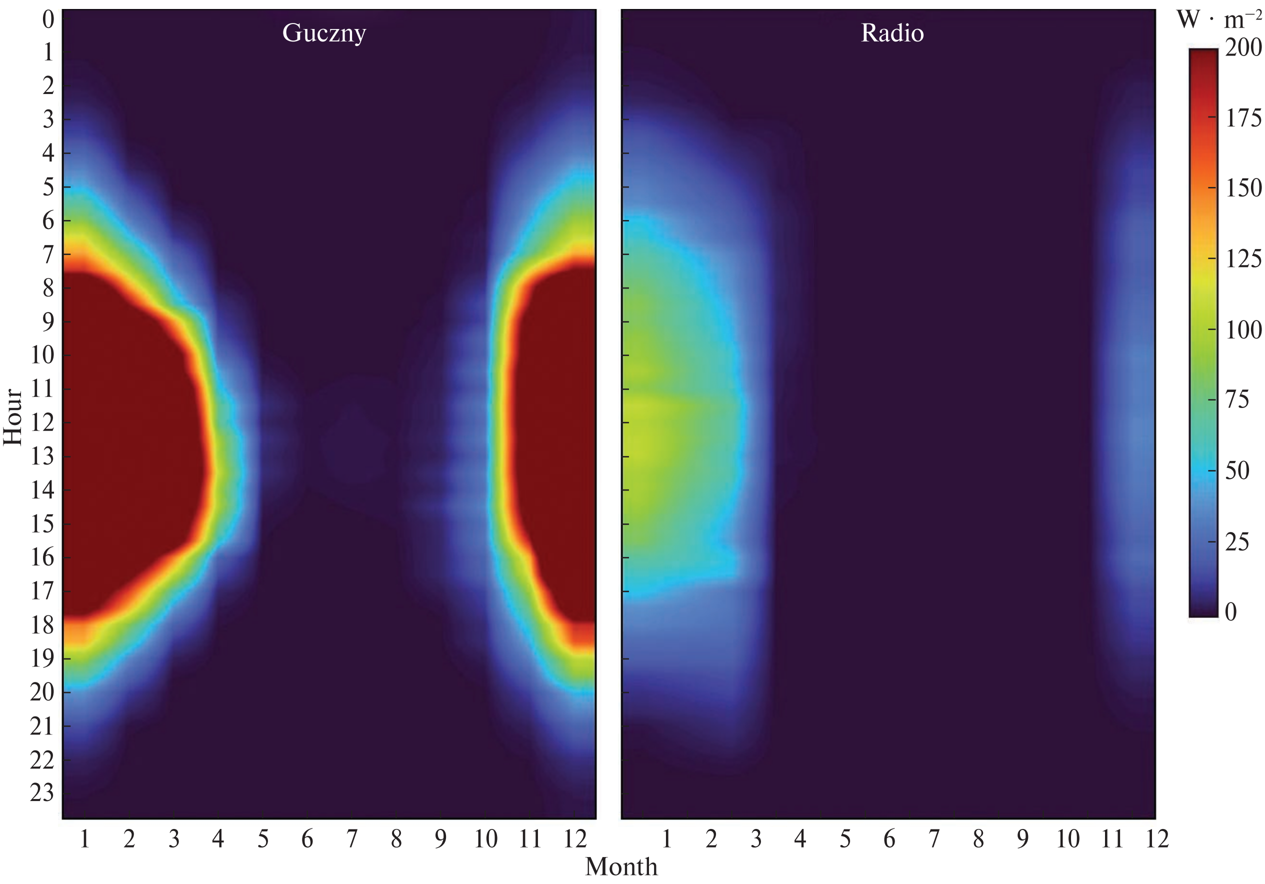

Figure 3. Intra-annual distribution of the multi-year mean diurnal cycle of incoming solar irradiance for loggers with the highest ("Guczny") and lowest ("Radio") values

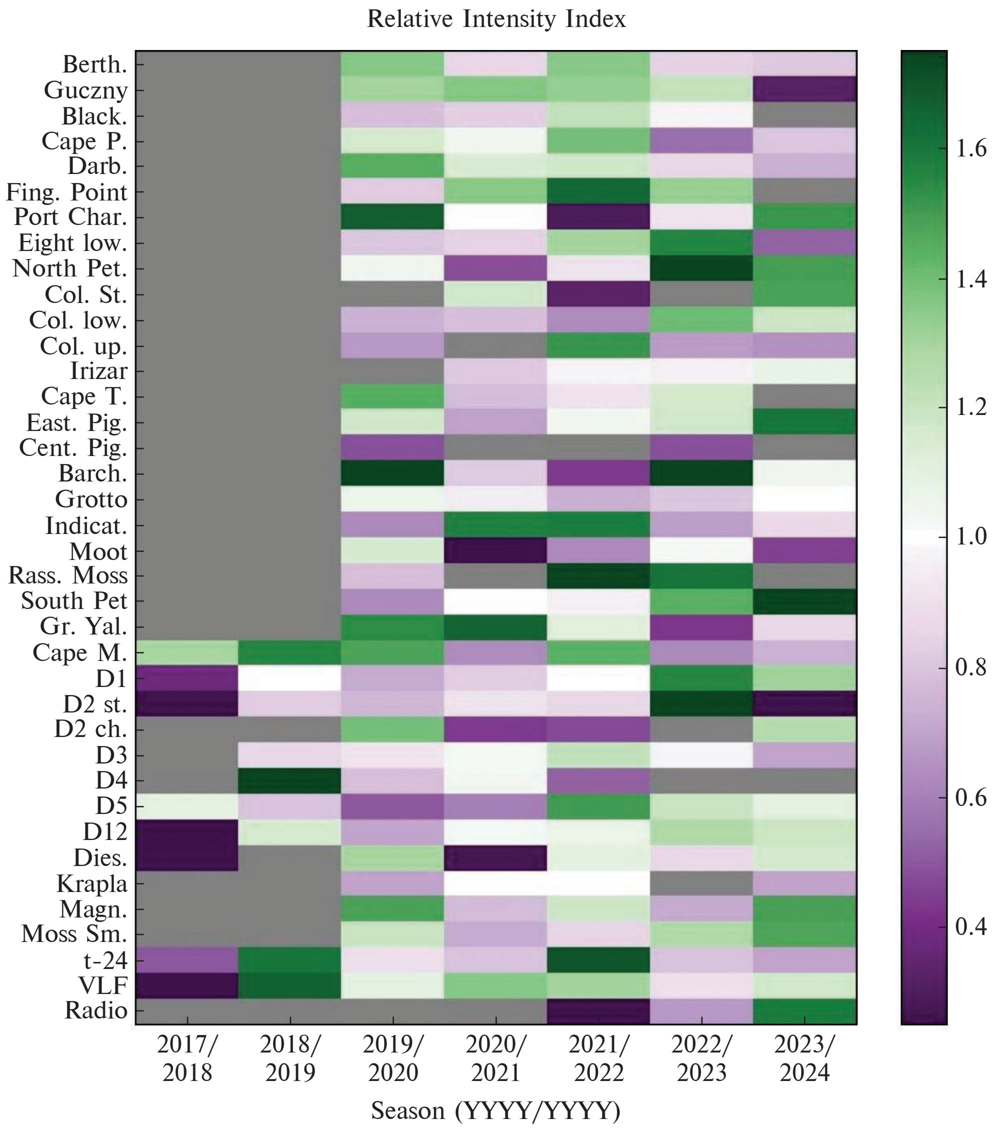

Figure 4. Interannual distribution of the Relative Intensity Index (grey colour indicates data absence or inability to calculate)

St.", "Barch.", and "Radio" loggers was 50–60% lower than the long-term mean values. At the same time, at the "Fing. Point", "Rass. Moss", "t-24," and several other loggers, this season was among the most highly irradiated, with mean values exceeding the long-term averages by 30–60%.

Nevertheless, general tendencies for the majority of loggers may still persist. For instance, a predominantly lower irradiance intensity is observed during the 2020/2021 season.

Unfortunately, the inability to calculate accumulated values from loggers' data, due to filtering out erroneous measurements, significantly limits the assessment of the actual radiation resources available to plants at microrelief sites. In any case, even under the hypothetical assumption of the absence of erroneous or overestimated irradiance values, the obtained results indicate the critical importance of evaluating horizon obstruction when studying microclimatic conditions in

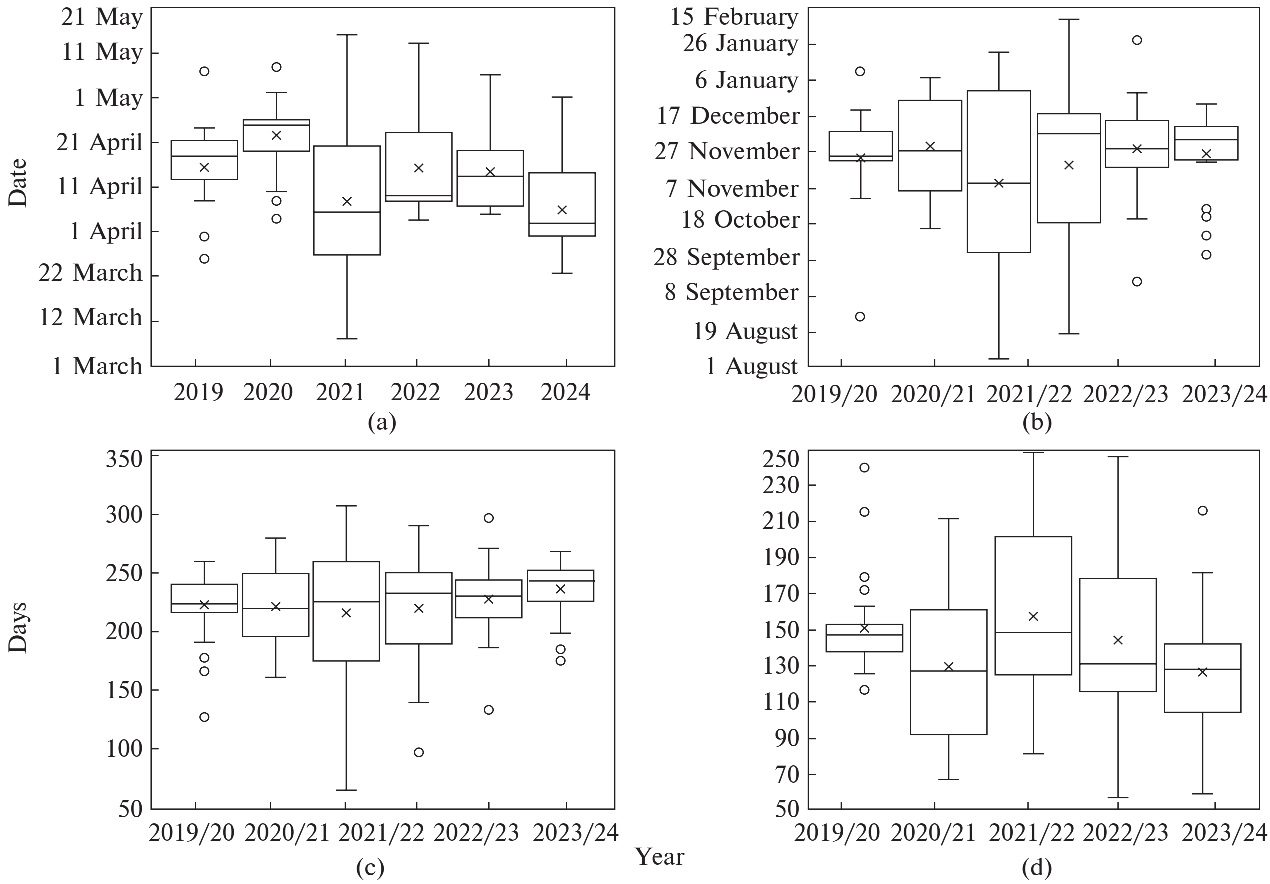

Figure 5. (a) — box-and-whisker plots showing dates of flux disappearance, (b) — flux appearance, (c) — duration of the season without incoming irradiance ("under snow"), (d) — duration of the season with daytime incoming irradiance ("no steady snow"). The mean is represented by a cross (×); the median is represented by a horizontal line within the box; outliers are represented by circular markers

Antarctica. Such data were recorded experimentally for the first time during the seasonal fieldwork of the 29th Ukrainian Antarctic Expedition in February—April 2025. Future processing of these data will determine a more accurate assessment of radiation resources available to plants, including a transition from purely statistical evaluation methods to the calculation of physical equations describing the integrated incoming solar radiation.

3.4 Logger-measured solar irradiance as an indicator of snow cover availability

The formation of a stable snow cover (*i.e.*, the disappearance of irradiance) generally occurs between late March and the second half of April (Fig. 5a). Within a single season, the disappearance of irradiance typically takes place over a period of 10—15 days. An exceptional case was 2021, which exhibited a very wide range in the timing of stable snow cover formation across studied locations, spanning nearly two months — from 10 March to 12 May.

Of particular interest is the shift in mean values over the period 2019—2024 (in Fig. 5a, averages are marked with crosses, while medians are shown as solid lines within the boxplots). The disappearance of irradiance tends to occur earlier, shifting from the second ten-day period of April to the first.

It is logical that the formation of a stable snow cover at different sites is largely controlled by an external factor — snowfall events that simultaneously cover large areas (relative to the size of the monitoring site). Under such conditions, the role of microclimatic variability is diminished, and differences in the timing of stable snow cover establishment generally occur within a single month. In contrast to the transition into the cold season, snowmelt occurs over much wider time ranges. During the transition from the cold to the warm season, microclimatic conditions become the determining factor. Thus, the disappearance of snow cover (*i.e.*, the reappearance of irradiance) in 2021 and 2022 began as early as the first half of August and extended until late January — mid-February of the following year (Fig. 5b). On average, the melting of the stable snow cover occurs during November. Thus, for most of the year, vegetation (and the nearby loggers) remains covered by snow, with the duration of this period averaging 220—230 days (Fig. 5c). During the study period, stable snow cover sometimes persisted for fewer than 100 days. The maximum recorded duration exceeded 300 days in 2021.

The period without stable snow cover (*i.e.*, with regular occurrence of daytime irradiance) lasts on average 130—150 days (Fig. 5d). Almost every year, there are sites where the snow-free period (without stable snow cover) is shorter than 90 days (Fig. 5, 6). The longest snow-free periods exceeded 230 days (Fig. 5, 6). However, it should be emphasised once again that this refers not to the total number of days with snow presence, but to the dates of stable formation and melting of the snow cover. During the warm season, snowfall events are frequent and may temporarily lead to snow accumulation, which, for short periods, blocks solar radiation from reaching loggers and vegetation. Duration of periods with daytime incoming solar irradiance for all loggers and seasons are presented in Table A2.

An attempt to compare differences in the stable formation and melting of snow cover between *C. quitensis* and *D. antarctica* did not yield statistically robust results (Fig. 7). The only notable difference is that the higher percentiles (above the 50th percentile) of the snow-free period duration for *C. quitensis* are 20—40 days longer (Fig. 7d). This indicates that the growth conditions of *C. quitensis* tend to be associated with sites that experience longer periods of irradiance than those of *D. antarctica*. Nevertheless, the overall variability remains similar for both species.

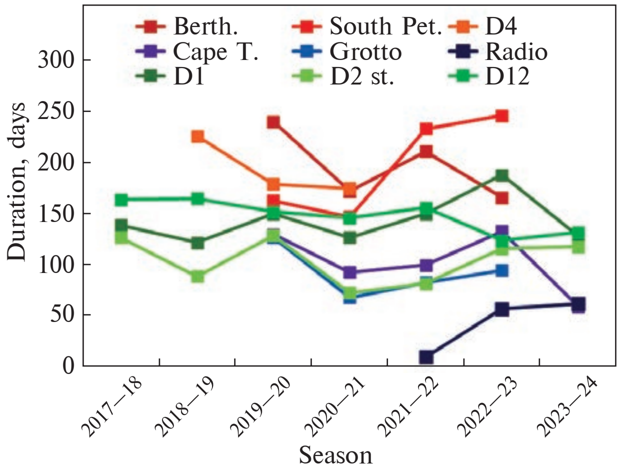

Figure 6. Temporal changes of the period with daytime incoming irradiance indicated the absence of steady snow cover on the example of loggers with the highest (“Berth.”, “South Pet.”, “D4”) and lowest (“Cape T.”, “Grotto”, “D2 st.”, “Radio”) mean values, and with the longest time series (“D1”, “D2 st.”, “D12”)

3.5 Discussion

The study presents the first assessment of incoming solar irradiance under such experimental conditions near native vascular plants in Antarctica across the Argentine Islands-Kyiv Peninsula area. Despite substantial differences from conventional meteorological measurements, the obtained mean values are consistent with those reported in standard actinometric observations. Depending on the monitoring site in Antarctica, reported summer short-wave incoming irradiance ranges from 400 to 500 W · m^{-2} in Dronning Maud Land (van den Broeke et al., 2004), about 380 W · m^{-2} on King George Island (Soares et al., 2019), over 300 W · m^{-2}

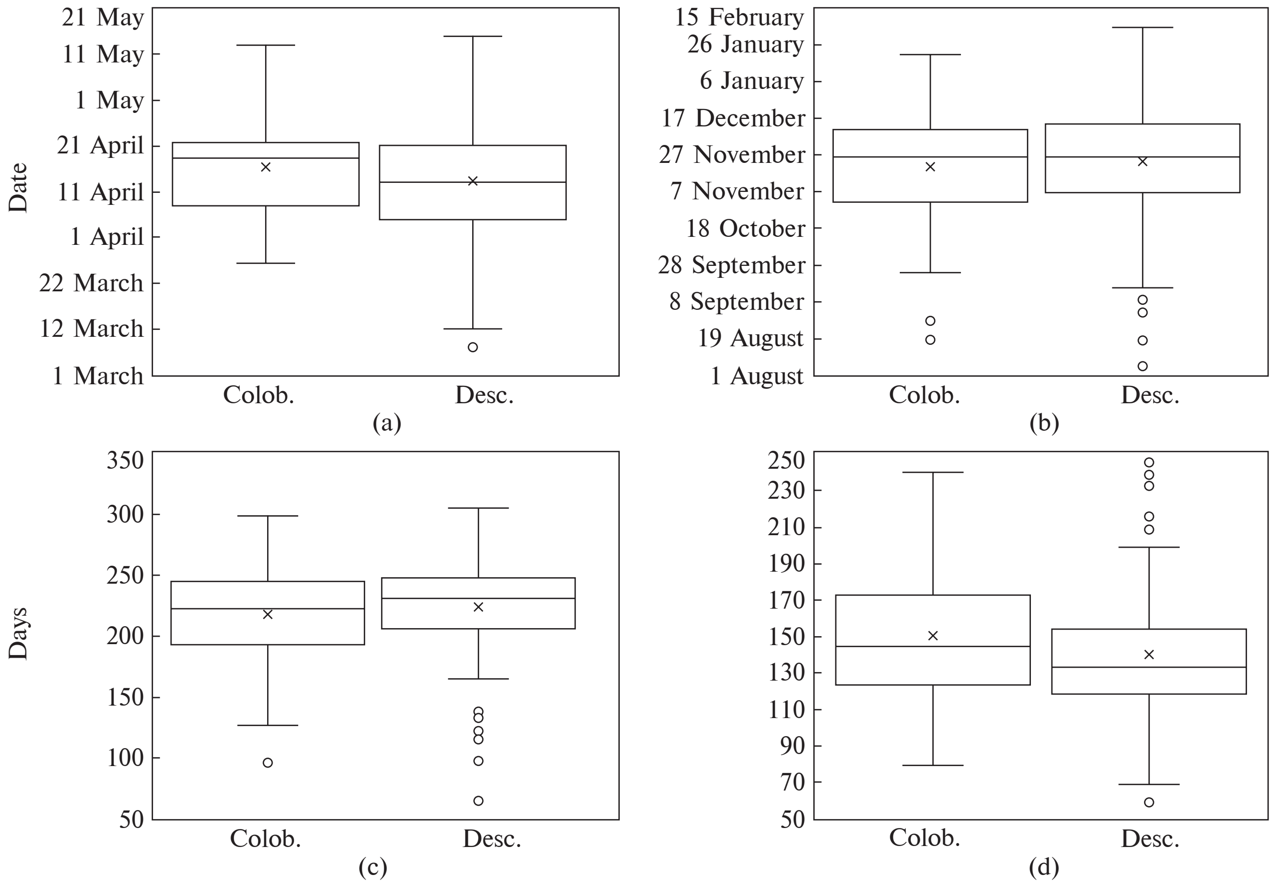

Figure 7. The comparison of box-and-whisker plots for *Colobanthus quitensis* ("Colob.") and *Deschampsia antarctica* ("Desc.") showing dates of flux disappearance (a), flux appearance (b), duration of the season without incoming irradiance ("under snow") (c), and duration of the season with daytime incoming irradiance ("no steady snow") (d). The mean is represented by a cross (×); the median is represented by a horizontal line within the box; outliers are represented by circular markers

at Dome C (Bai et al., 2022), and approximately 470 W · m^{-2} over landfast sea ice near Zhongshan Station (Yu et al., 2019). At the Vernadsky Station, global solar radiation of up to 400 W · m^{-2} was recorded (Láska et al., 2009). In our study, summer incoming solar irradiance varied between 200 and 500 W · m^{-2}, despite being measured at the microscale under a strong influence of terrain. The obtained average annual values are also consistent with other measurements, for example, those from the McMurdo Dry Valleys, where values between 84 and 117 W · m^{-2} were reported (Dana et al., 1998).

A similar consistency is observed for maximum values. The far-southern Mario Zucchelli Station, located in Terra Nova Bay, recorded incoming solar radiation reaching up to 1000 W · m^{-2} (Balog et al., 2019), indicating that instantaneous irradiance values can reach very high levels. These values directly affect native vascular plants near the surface and also demonstrate the potential for sensor "saturation" effects under Antarctic conditions. In our study, quality control procedures identified more than 11000 theoretically impossible overestimated irradiance values, reaching up to 1.6% of all measurements at some loggers. Although this represents a relatively small proportion of the dataset, the absolute magnitudes of these values are sufficiently high to bias statistical analyses and therefore must be filtered. We recommend that future studies also filter the corresponding temperature data when such irradiance anomalies are detected, as under these conditions, the sensor is unable to record realistic environmental parameters.

In terms of snow cover, surface irradiance measurements near native vascular plants can serve as a reliable indicator of snow cover availability. The timing of stable snow cover formation is consistent with recent results reported by Shpyg et al. (2024) for Galindez Island. Although the average transition to the warm season is close to that observed in standard meteorological measurements, microscale differences in snowmelt timing are substantial. The latest estimations showed that the duration of snowmelt ranged from 50 to 117 days based on standard meteorological observations (Khrystiuk et al., 2026). This represents a significantly lower range compared to areas where native vascular plants occur, which experience, on average, 130—150 snow-free days per year, with a total range typically between 90 and 200 days.

At the microscale, snow parameters can be highly variable, depending not only on weather conditions but also on microscale terrain features, wind fields modified by these features, and even land cover type (Tarca et al., 2022). Hence, the need to identify snow cover at the microscale has already been highlighted not only in terms of its impact on local vegetation but also for tracking the effects of climate change on Antarctic ecosystems.

While the presented results demonstrate the potential of surface logger irradiance measurements to serve as a proxy parameter for identifying snow cover presence and melting in remote regions, future studies should verify these findings using fully equipped microclimatological stations. Such observations would allow determination of exact irradiance thresholds, or ranges of values, that could be used to identify the transition from initial snow formation to the establishment of stable snow cover.

Comparing the differences in the stable formation and melting of snow cover between *C. quitensis* and *D. antarctica* shows their overall similarity for both species. These results seem to confirm that the significantly lower prevalence of *C. quitensis* in the studied region compared to *D. antarctica* is not related to micro-conditions, but rather to the more problematic dispersal of the former. The observed differences may reflect the combined effects of additional factors, such as elevation and climatic conditions (Cannone et al., 2016). However, it should be emphasised that the microscale irradiance variability is far more heterogeneous than suggested by spatially averaged parameters. Moreover, microscale variability may exhibit patterns that are opposite to those inferred from standard meteorological observations. We demonstrate that the same season can be considerably more illuminated at some locations, while irradiance at others remains below their multi-seasonal average. Although some sensors may have been affected by local fauna (primarily by gentoo penguins, which spread their nesting area across the region) or by shading caused by changes in sensor positioning, the spatial extent of the observed variability and the number of sites exhibiting contrasting patterns indicate that these effects are not random. Instead, they reflect persistent microscale conditions specific to individual locations. Some sites consistently receive higher irradiance than others, with snow cover accounting for a substantial portion of these differences. Large temporal differences in snowmelt timing therefore drive the observed variability in solar irradiance reaching the surface where vascular plants are located. Since vascular plants are affected by both average temperatures and the positive temperatures accumulation, although often in different ways (Miryuta et al., 2025), important factors that indirectly affect both temperature indices are light intensity and season length, which directly depends on the snow-free period length.

4 Conclusions

We found out that mean near-noon incoming solar irradiance conditions during the Antarctic summer in the Argentine Islands-Kyiv Peninsula region typically range between 200 and 500 $W \cdot m^{-2}$, although some instantaneous values can exceed 1000 $W \cdot m^{-2}$. Intense incoming solar irradiance is observed during summer, between 07:00 and 18:30 local (UTC-4) time, and disappears after the formation of a stable snow cover from April to October. No statistically robust differences in the intra-annual irradiance cycle were detected between *Colobanthus quitensis* and *Deschampsia antarctica*. Although the minimum mean irradiance values for *C. quitensis* are higher than those for *D. antarctica*, this variability may simply reflect the broader spatial coverage of loggers deployed at *D. antarctica* sites.

Despite similar external conditions of incoming solar irradiance and atmospheric attenuation, micro-scale environmental variability can lead to substantial differences even between neighbouring logger sites. In particular, analysis of inter-seasonal distribution showed that distinct irradiance conditions may develop at specific sites within the same season. Simultaneously, irradiance at different sites may deviate by up to ±60% from long-term mean values.

Microclimatic conditions exert a strong influence on snowmelt, whereas snow cover formation is predominantly controlled by external factors, particularly widespread snowfall events. The disappearance of irradiance (*i.e.*, the formation of stable snow cover) most commonly occurs in April and typically encompasses all study sites within a single month. In contrast, the reappearance of regular daytime irradiance (*i.e.*, melting of the stable snow cover) may span more than half a year, although most cases occur during November. Incoming solar irradiance measured by loggers near native vascular plants can serve as a proxy for seasonal conditions and be compared with biological parameters of plant dynamics.

As expected, stable snow-cover period lasts longer, averaging 220—230 days, whereas the snow-free period averages 130—150 days. Native vascular plants were found to grow mainly during 90 to 200 days of the snow-free period, and these variations depend more on local site characteristics than on meteorological variability. Differences in the timing of stable snow cover formation/melt and in the duration of these periods between plant species do not yield statistically robust results. Nevertheless, certain patterns in irradiance variability suggest that *C. quitensis* may preferentially occupy sites with longer periods of irradiance.

Author contributions. Idea, conceptualisation: M. S. Data preparation and processing: M. S., L. P., N. M., I. P, A. P, D. P., visualisation: M. S. Initial draft: M. S. Writing: M. S., L. P., D. P., I. P.

Acknowledgements. Authors thank all biologists of Ukrainian Antarctic expeditions who assist in maintaining the Bio-microclimatic Monitoring Site.

Funding. This research was conducted within the framework of the State Special-Purpose Research Program in Antarctica for 2011—2027.

Conflict of Interest. The authors declare no conflict of interest.

References

Andrade, A. M. de, Michel, R. F. M., Bremer, U. F., Schaefer, C. E. G. R., & Simxes, J. C. (2018). Relationship between solar radiation and surface distribution of vegetation in Fildes Peninsula and Ardley Island, Maritime Antarctica. *International Journal of Remote Sensing*, *39*(8), 2238—2254. https://doi.org/10.1080/01431161.2017.1420937

Bai, J., Zong, X., Lanconelli, C., Lupi, A., Driemel, A., Vitale, V., Li, K., & Song, T. (2022). Long-Term Variations of Global Solar Radiation and Its Potential Effects at Dome C (Antarctica). *International Journal of Environmental Research and Public Health*, *19*(5), 3084. https://doi.org/10.3390/ijerph19053084

Balog, I., Spinelli, F., Grigioni, P., Caputo, G., Napoli, G., & de Silvestri, L. (2019). Estimation of Direct Normal Irradiance at Antarctica for Concentrated Solar Technology. *Applied System Innovation*, *2*(3), 21. https://doi.org/10.3390/asi2030021

Barrera, A., Hereme, R., Ruiz-Lara, S., Larrondo, L. F., Gundel, P. E., Pollmann, S., Molina-Montenegro, M. A., & Ramos, P. (2020). Fungal Endophytes Enhance the Photoprotective Mechanisms and Photochemical Efficiency in the Antarctic *Colobanthus quitensis* (Kunth) Bartl. Exposed to UV-B Radiation. *Frontiers in Ecology and Evolution*, *8*, 122. https://doi.org/10.3389/fevo.2020.00122

Cannone, N., Guglielmin, M., Convey, P., Worland, M. R., & Favero Longo, S. E. (2016). Vascular plant changes in extreme environments: effects of multiple drivers. *Climatic Change*, *134*, 651—665. https://doi.org/10.1007/s10584-015-1551-7

Dana, G. L., Wharton, R. A., Jr., & Dubayah, R. A. (1998). Solar Radiation in the Mcmurdo Dry Valleys, Antarctica. In J. C. Priscu (Ed.), *Ecosystem Dynamics in a Polar Desert: the Mcmurdo Dry Valleys, Antarctica* (pp. 39–64). https://doi.org/10.1029/AR072p0039

Day, T. A., Ruhland, C. T., & Xiong, F. S. (2001). Influence of solar ultraviolet-B radiation on Antarctic terrestrial plants: results from a 4-year field study. *Journal of Photochemistry and Photobiology B: Biology*, *62*(1–2), 78–87. https://doi.org/10.1016/S1011-1344(01)00161-0

di Carmine, C., Campanelli, M., Nakajima, T., Tomasi, C., & Vitale, V. (2005). Retrievals of Antarctic aerosol characteristics using a Sun-sky radiometer during the 2001–2002 austral summer campaign. *Journal of Geophysical Research: Atmospheres*, *110*(D13), D13202. https://doi.org/10.1029/2004JD005280

Ding, M., Agrawal, A., Heil, P., & Yang, D. (2019). Surface energy balance on the Antarctic plateau as measured with an automatic weather station during 2014. *Advances in Polar Science*, *30*(2), 93–105. https://doi.org/10.13679/j.advps.2018.0050 https://library.arcticportal.org/2685/1/A1902002.pdf

Katurji, M., Zawar-Reza, P., & Zhong, S. (2013). Surface layer response to topographic solar shading in Antarctica's dry valleys. *Journal of Geophysical Research: Atmospheres*, *118*(22), 12,332–12,344. https://doi.org/10.1002/2013JD020530

Khrystiuk, B., Gorbachova, L., Shpyg, V., Pishniak, D., & Klok, S. (2026). Estimation of snow cover melting characteristics from Vernadsky weather station data (Antarctica). *Meteorology Hydrology and Water Management*, *14*(1), 106–118. https://doi.org/10.26491/mhwm/217541

Láska, K., Prošek, P., Budík, L., Budíková, M., & Milinevsky, G. (2009). Prediction of erythemally effective UVB radiation by means of nonlinear regression model. *Environmetrics*, *20*(6), 633–646. https://doi.org/10.1002/env.968

Matos, P., Rocha, B., Pinho, P., Miranda, V., Pina, P., Goyanes, G., & Vieira, G. (2024). Microscale is key to model current and future Maritime Antarctic vegetation. *Science of The Total Environment*, 946, 174171. https://doi.org/10.1016/j.scitotenv.2024.174171

Miryuta, N., Parnikoza, I., Oliinyk, M., Smetana, E., Myryuta, G., Poronnik, O., & Kunakh, V. (2017). Five seasons dynamic of adaptability united latent quality indicator of *Deschampsia antarctica* (Poaceae) population of Galindez Island (Argentine Islands, maritime Antarctic). *Ukrainian Antarctic Journal*, (16), 129–142. https://doi.org/10.33275/1727-7485.16.2017.71

Miryuta, N., Savenets, M., Pysarenko, L., Myryuta, G., Poronnik, O., & Parnikoza, I. (2025). Spatio-temporal variability of soil surface temperature affects adaptation of Antarctic hairgrass populations. 1. Fluctuations of average monthly local temperature near plants influence biometrical, biochemical, and ecological characteristics. *Czech Polar Reports*, *15*(2), 285–302. https://doi.org/10.5817/CPR2025-2-17

Obryk, M. K., Fountain, A. G., Doran, P. T., Lyons, W. B., & Eastman, R. (2018). Drivers of solar radiation variability in the McMurdo Dry Valleys, Antarctica. *Scientific Reports*, *8*(1), 5002. https://doi.org/10.1038/s41598-018-23390-7

Pannewitz, S., Schlensog, M., Allan Green, T. G., Sancho, L. G., & Schroeter, B. (2003). Are Lichens Active under Snow in Continental Antarctica? *Oecologia*, *135*(1), 30–38. https://www.jstor.org/stable/4223554

Petkov, B. H., Láska, K., Vitale, V., Lanconelli, C., Lupi, A., Mazzola, M., & Budíková, M. (2016). Variability in solar irradiance observed at two contrasting Antarctic sites. *Atmospheric Research*, *172–173*, 126–135. https://doi.org/10.1016/j.atmosres.2016.01.005

Raggio, J., Green, T. G. A., & Sancho, L. G. (2016). *In situ* monitoring of microclimate and metabolic activity in lichens from Antarctic extremes: a comparison between South Shetland Islands and the McMurdo Dry Valleys. *Polar Biology*, *39*(1), 113–122. https://doi.org/10.1007/s00300-015-1676-1

Ramírez, C. F., Cavieres, L. A., Sanhueza, C., Vallejos, V., Gómez-Espinoza, O., Bravo, L. A., & Sáez, P. L. (2024). Ecophysiology of Antarctic Vascular Plants: An Update on the Extreme Environment Resistance Mechanisms and Their Importance in Facing Climate Change. *Plants*, *13*(3), 449. https://doi.org/10.3390/plants13030449

Savenets, M., Pysarenko, L., Krakovska, S., Parnikoza, I., & Pishniak, D. (2023). Local temperature near native vascular plants in the Argentine Islands–Kyiv Peninsula region, Antarctic Peninsula: annual variability and approximation using standard meteorological measurements. *Polar Research*, *42*, 8339. https://doi.org/10.33265/polar.v42.8339

Schroeter, B., Green, T. G. A., Pannewitz, S., Schlensog, M., & Sancho, L. G. (2011). Summer variability, winter dormancy: lichen activity over 3 years at Botany Bay, 77°S latitude, continental Antarctica. *Polar Biology*, *34*(1), 13–22. https://doi.org/10.1007/s00300-010-0851-7

Shpyg, V., Shchehlov, O., & Pishniak, D. (2024). Snow cover at the Akademik Vernadsky station: response on wind, temperature and precipitation variations. *Ukrainian Antarctic Journal*, *22*(1(28), 6–23. https://doi.org/10.33275/1727-7485.1.2024.724

Soares, J., Alves, M., Ribeiro, F. N. D., & Codato, G. (2019). Surface radiation balance and weather conditions on a non-glaciated coastal area in the Antarctic region. *Polar Science*, *20(2)*, 117–128. https://doi.org/10.1016/j.polar.2019.04.001

Stanhill, G., & Cohen, S. (1997). Recent Changes in Solar Irradiance in Antarctica. *Journal of Climate*, *10*(8), 2078–2086. https://doi.org/10.1175/1520-0442(1997)010<2078:RCISII>2.0.CO;2.

Szymszová, S., Láska, K., Kim, S.-J., & Park, S.-J. (2025). Variability of solar radiation and cloud cover in the Antarctic Peninsula region. *Atmospheric Research*, *316*, 107940. https://doi.org/10.1016/j.atmosres.2025.107940

Tarca, G., Guglielmin, M., Convey, P., Worland, M. R., & Cannone, N. (2022). Small-scale spatial-temporal variability in snow cover and relationships with vegetation and climate in maritime Antarctica. *CATENA*, *208*, 105739. https://doi.org/10.1016/j.catena.2021.105739

van den Broeke, M., Reijmer, C., & van de Wal, R. (2004). Surface radiation balance in Antarctica as measured with automatic weather stations. *Journal of Geophysical Research: Atmospheres*, *109*(D9). https://doi.org/10.1029/2003JD004394

Yevchun, H., Fedchuk, A., Drohushevska, I., Pnyovska, O., Chernyshenko, M., & Parnikoza, I. (2021). The Toponymy of the Argentine Islands area, the Kyiv Peninsula (West Antarctica). *Ukrainian Antarctic Journal*, (2), 127—157. https://doi.org/10.33275/1727-7485.2.2021.683

Yu, L., Yang, Q., Zhou, M., Lenschow, D. H., Wang, X., Zhao, J., Sun, Q., Tian, Z., Shen, H., & Zhang, L. (2019). The variability of surface radiation fluxes over landfast sea ice near Zhongshan station, east Antarctica during austral spring. *International Journal of Digital Earth*, *12*(8), 860–877. https://doi.org/10.1080/17538947.2017.1304458

Zeng, Z., Wang, X., Wang, Z., Zhang, W., Zhang, D., Zhu, K., Mai, X., Cheng, W., & Ding, M. (2022). A 35-year daily global solar radiation dataset reconstruction at the Great Wall Station, Antarctica: First results and comparison with ERA5, CRA40 reanalysis, and ICDR (AVHRR) satellite products. *Frontiers in Earth Science*, *10*, 961799. https://doi.org/10.3389/feart.2022.961799

Zhang, T., Zhou, C., & Zheng, L. (2019). Analysis of the temporal-spatial changes in surface radiation budget over the Antarctic sea ice region. *Science of The Total Environment*, *666*, 1134–1150. https://doi.org/10.1016/j.scitotenv.2019.02.264

Received: 16 February 2026
Accepted: 1 June 2026
Published: 3 July 2026

Мікрокліматична мінливість притоку сонячної радіації та наявності снігового покриву поблизу аборигенних судинних рослин морської Антарктики

Михайло Савенець[1, *], Лариса Писаренко[1, 2], Антон Пуговкін[2, 3, 4, 5], Наталія Мірюта[2], Денис Пішняк[2], Іван Парнікоза[2, 6]

[1] Український гідрометеорологічний інститут Державної служби України з надзвичайних ситуацій та Національної академії наук України, м. Київ, 03028, Україна
[2] Державна установа Національний антарктичний науковий центр Міністерства освіти і науки України, м. Київ, 01601, Україна
[3] Університет Масарика, відділ географії, м. Брно, 61137, Чеська Республіка
[4] Університет Масарика, відділ експериментальної біології, м. Брно, 62500, Чеська Республіка
[5] Інститут проблем кріобіології і кріомедицини НАН України, м. Харків, 61016, Україна
[6] Національний історико-архітектурний музей «Київська фортеця», м. Київ, 01133, Україна

*** Автор для кореспонденції:** savenets@uhmi.org.ua, savenetsm@gmail.com

Реферат. Прихідний потік сонячного випромінювання є важливим фактором виживання місцевих судинних рослин Антарктики, який формує основне джерело енергії для місцевої наземної рослинності. Нами проаналізовано мікрокліматичну мінливість притоку сонячного випромінювання до земної поверхні та оцінено придатність до використання у якості проксі-параметра з метою ідентифікації наявності снігового покриву у віддалених регіонах. Дослідження проведені на основі мережі 38 логерів температури та освітленості на полігоні, що охоплює район Аргентинських островів – півострова Київ, за період 2017–2025 рр. У масштабі мікроумов, де поширені *Colobanthus quitensis* та *Deschampsia antarctica*, типові середні літні значення сонячної радіації складають 200–500 В · м$^{-2}$, з відхиленнями до ±60% від середніх багаторічних значень через мікрокліматичні особливості. Ми проаналізували періоди з майже нульовою освітленістю, яка вказує на стійкий сніговий покрив, що типово спостерігається у період з квітня по жовтень. Будучи виміряним біля поверхні, зникнення сонячного випромінювання може слугувати проксі-параметром наявності снігового покриву. Дати формування стійкого снігового покриву були близькі, а дати танення – значно відмінні. У місцях поширення місцевих судинних рослин період без снігу варіює в межах від 90 до 200 днів та залежить від мікрокліматичних особливостей. Не було виявлено статистично надійних різниць показників річного циклу притоку сонячної радіації між локаціями з *C. quitensis* and *D. antarctica*. Проте виявлено, що для перлинниці більш типовими ділянками можуть бути ті, які характеризуються довшим періодом освітленості. Проведені дослідження наголошують на необхідності врахування притоку сонячного випромінювання безпосередньо в мікромасштабі та показують потенціал сенсорів освітленості до використання у якості проксі-параметру оцінки наявності снігового покриву у віддалених районах Антарктики, де неможливо проводити інші прямі спостереження.

Ключові слова: Антарктика, інтенсивність освітлення, мікроклімат, перлинниця антарктична, танення снігу, щучник антарктичний

APPENDIX

Table A1. List of loggers of Bio-microclimatic Monitoring Site of Argentine Islands-Kyiv Peninsula region

№	Short name*	Location**	Plant species	Latitude, °	Longitude, °
1	Cape M.	Magnit Point, Galindez Island, Argentine Islands	*D. antarctica*	−65.245	−64.2531
2	Col. low.	Colobanthus, lower point, near the Antarctic pearlwort, Roztochchia Ridge, Galindez Island, Argentine Islands	*C. quitensis, D. antarctica*	−65.247967	−64.242600
3	Col. up.	Colobanthus, upper point, near the Antarctic pearlwort, Roztochchia Ridge, Galindez Island, Argentine Islands	*C. quitensis, D. antarctica*	−65.247917	−64.242583
4	D1	Near meteorological station, Meteo Point, Marina Point, Galindez Island, Argentine Islands	*D. antarctica*	−65.2448	−64.2558
5	D2 st.	near main station building (Coronation House), Marina Point, Galindez Island, Argentine Islands	*D. antarctica*	−65.2457	−64.2575
6	D2 ch.	D2—OTC, open top chamber, near main station building (Coronation House), Marina Point, Galindez Island, Argentine Islands	*C. quitensis, D. antarctica*	−65.2457	−64.2575
7	D3	Leopard Tower, Penguin Point, Galindez Island, Argentine Islands	*D. antarctica*	−65.2475	−64.2401
8	D4	Korabel Rock, Penguin Point, Galindez Island, Argentine Islands	*D. antarctica*	−65.2486	−64.2382
9	D5	Woozle Hill, the upper terrace of the Hovorukha dome under the Anna Hill, Galindez Island, Argentine Islands	*D. antarctica*	−65.2483	−64.2454
10	D12	On the Gull Tower slopes on Stella Point, Galindez Island, Argentine Islands	*D. antarctica*	−65.2474	−64.2526
11	Dies.	Near Diesel hut, Galindez Island, Argentine Islands	*D. antarctica*	−65.2459	−64.2581
12	Krapla	Krapla Rock, Galindez Island, Argentine Islands	*D. antarctica*	−65.2469	−64.2441
13	Magn.	Magnit hut, Galindez Island, Argentine Islands	*D. antarctica*	−65.2453	−64.251
14	Moss. Sm.	Moss Valley, Smith moss bank, Galindez Island	*D. antarctica*	−65.2477	−64.2508
15	Radio	Near Radiomast, Marina Point, Galindez Island, Argentine Islands	absent	−65.2462	−64.2549
16	t—24	On the rocky shore of the Shya Ridge behind the large magnetic pavilion	*D. antarctica*	−65.2453	−65.2453
17	VLF	On the Cemetry Ridge near the pavilion of Very Low Frequencies (VLF), Galindez Island, Argentine Islands	*D. antarctica*	−65.246137	−64.248816
18	Col. St.	Colobanthus locus, near station, Galindez Island	*C. quitensis*	−65.245602	−64.257024

End of Table A1

№	Short name*	Location**	Plant species	Latitude, °	Longitude, °
19	Black.	Black Island, Argentine Islands	*C. quitensis, D. antarctica*	−65.258	−64.2806
20	Cape P.	Western Point, Cape Perez	*C. quitensis*	−65.4076	−64.0971
21	Cape T.	Moss bank, Cape Tuxen	*D. antarctica*	−65.2681	−64.1165
22	Cent. Pig.	Central Pig Island, Argentine Islands	*D. antarctica*	−65.2429	−64.2737
23	Darb.	Encalypta (NE) Point, Darboux Island	*C. quitensis, D. antarctica*	−65.3952	−64.2149
24	East. Pig.	Eastern Pig Island, Argentine Islands	*D. antarctica*	−65.2434	−64.2699
25	Eight low.	Lower locus on Eight Island, Argentine Islands	*C. quitensis, D. antarctica*	−65.2257	−64.2096
26	Fing. Point	Finger Point of Skua Island, Argentine Islands	*C. quitensis, D. antarctica*	−65.2552	−64.2747
27	Gr. Yal.	Great Yalour Island	*D. antarctica*	−65.2344	−64.1622
28	Grotto	Grotto Island, Argentine Islands	*D. antarctica*	−65.2424	−64.2476
29	Guczny	Huchnyi Island, Argentine Islands	*C. quitensis*	−65.2344	−64.2165
30	Indicat.	Indicator Island, Argentine Islands	*D. antarctica*	−65.2459	−64.2638
31	Irizar	Irizar Island, Argentine Islands	*C. quitensis, D. antarctica*	−65.219	−64.2001
32	Moot	(a) Moot Island to 2022; (b) nearest Moot Point since 2022	*D. antarctica*	(a) −65.2055 (b) −65.203718	(a) −64.0799 (b) −64.074232
33	North Pet.	North part of Petermann Island	*C. quitensis, D. antarctica*	−65.165833	−64.140772
34	Port Char.	Port Charcot, Booth Island	*D. antarctica*	−65.067496	−64.015060
35	Rass. Moss	Rasmussen Point	*D. antarctica*	−65.2471	−64.0856
36	South Pet.	South part of Petermann Island	*D. antarctica*	−65.1747	−64.1412
37	Barch.	The biggest of The Barchans (Bondarchuk Island), Argentine Islands	*D. antarctica*	−65.241542	−64.301269
38	Berth.	The biggest of the Berthelot Islands (Ukraine Island)	*D. antarctica*	−65.329090	−64.161650

* Short names of loggers are provided according to Savenets et al. (2023).
** The local toponyms are provided according to Yevchun et al. (2021).

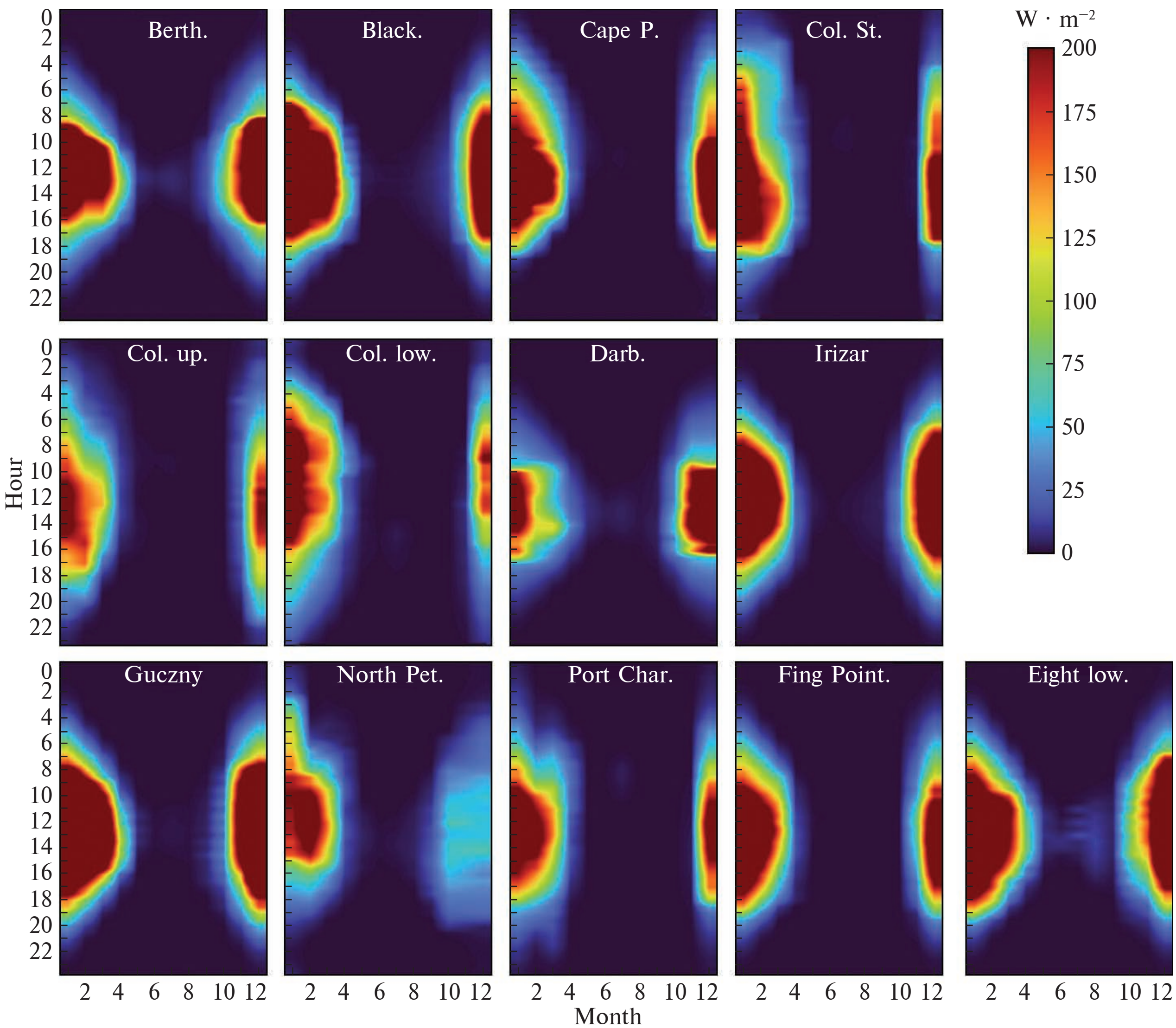

Figure A1. Intra-annual distribution of the multi-year mean diurnal cycle of incoming solar irradiance for loggers located on *Colobanthus quitensis* stands

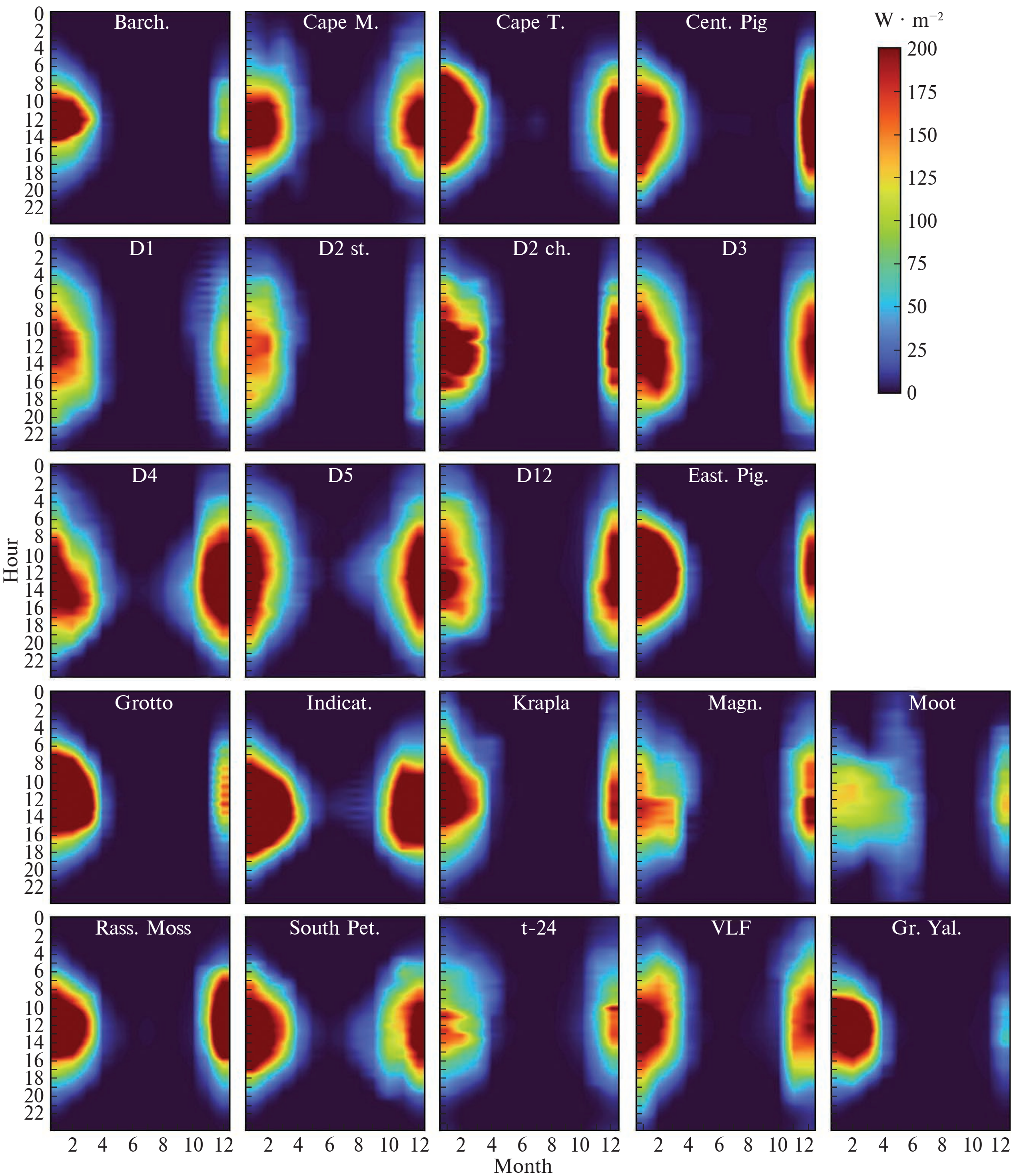

Figure A2. Intra-annual distribution of the multi-year mean diurnal cycle of incoming solar irradiance for loggers located on *Deschampsia antarctica* stands

Table A2. Temporal changes of the period with daytime incoming irradiance indicated the absence of steady snow cover

№	Short name	2017–2018	2018–2019	2019–2020	2020–2021	2021–2022	2022–2023	2023–2024
1	Cape M.	204	184	179	182	219	176	133
2	Col. low.			147	131	132	130	101
3	Col. up.			133	122		141	135
4	D1	139	122	150	127	150	188	128
5	D2 st.	127	89	129	73	82	116	118
6	D2 ch.			138	86			121
7	D3		137	152	120	150	121	123
8	D4		226	179	175			
9	D5	101	198	152	212	248	199	181
10	D12	164	165	152	146	156	124	132
11	Dies.			147	86	144	118	95
12	Krapla			145	91	130		
13	Magn.			148	132			133
14	Moss. Sm.			151	127	164	147	143
15	Radio					10	57	62
16	t-24							
17	VLF	54	176	152	169	219	178	155
18	Col. St.			148	103			141
19	Black.			140	155	205	137	
20	Cape P.			146	126	149	106	
21	Cape T.			130	93	100	133	59
22	Cent. Pig.			145			115	
23	Darb.			215	184	185	176	165
24	East. Pig.			139	85	134	107	
25	Eight low.			150	145	221	207	138
26	Fing. Point			144	119	146	120	
27	Gr. Yal.			126	132	90	60	115
28	Grotto			127	68	83	95	
29	Guczny			172	166	173	207	154
30	Indicat.			146	209	239	129	216
31	Irizar				139	192	180	
32	Moot			151		145	126	
33	North Pet.			117	79	123	240	97
34	Port Char.			142	96	91	115	109
35	Rass. Moss					175	141	123
36	South Pet.			163	147	233	246	
37	Barch.			127	80	98	123	91
38	Berth.			240	172	211	166	